Evaluation of the Reactive Power Support Capability and Associated Technical Costs of Photovoltaic Farms' Operation

Luís Lourenço, Renato Monaro, Mauricio Salles, Jose Cardoso, Loic Queval

energies

MDPI

Article

Evaluation of the Reactive Power Support Capability and Associated Technical Costs of Photovoltaic Farms' Operation

Luís F. N. Lourenço [1,*,†], Renato M. Monaro [1], Maurício B. C. Salles [1], José R. Cardoso [1] and Loïc Quéval [2]

[1] Laboratory of Advanced Electric Grids (LGRID), Escola Politécnica, University of São Paulo, São Paulo 05508-010, Brazil; monaro@usp.br (R.M.M.); mausalles@usp.br (M.B.C.S.); jose.cardoso@usp.br (J.R.C.)

[2] Group of Electrical Engineering—Paris (GeePs), UMR CNRS 8507, Centrale Supélec, Univ. Paris-Sud, Université Paris-Saclay, Sorbonne Université, 3 & 11 rue Joliot-Curie, 91192 Plateau de Moulon Gif-sur-Yvette CEDEX, France; loic.queval@geeps.centralesupelec.fr

* Correspondence: lfnlourenco@usp.br; Tel.: +55-11-3091-5533

† Current address: Av. Prof. Luciano Gualberto, 158-Butantã, São Paulo 05508-900, Brazil.

Received: 15 April 2018; Accepted: 8 June 2018; Published: 14 June 2018

Abstract: The share of photovoltaic (PV) farms is increasing in the energy mix as power systems move away from conventional carbon-emitting sources. PV farms are equipped with an expensive power converter, which is, most of the time, used well bellow its rated capacity. This has led to proposals to use it to provide reactive power support to the grid. In this framework, this work presents a step-by-step methodology to obtain the reactive power support capability map and the associated technical costs of single- and two-stage PV farms during daytime operation. Results show that the use of two-stage PV farms can expand the reactive power support capability for low irradiance values in comparison to single-stage ones. Besides, despite losses being higher for two-stage PV farms, the technical cost in providing reactive power support is similar for both systems. Based on the obtained maps, it is demonstrated how the profits of a PV farm can be evaluated for the current ancillary services policy in Brazil. The proposed method is of interest to PV farm owners and grid operators to estimate the cost of providing reactive power support and to evaluate the economic feasibility in offering this ancillary service.

Keywords: solar farm; photovoltaics; reactive power support; STATCOM; technical costs

1. Introduction

Utility-scale photovoltaic (PV) farms are expected to reach an installed capacity of 290 GW by 2019 [1]. This motivates the evolution of grid codes to regulate their connection to the electric grid. In particular, the reactive power support from PV farms is being discussed in many countries [2], and updates are expected from early grid codes that prevented them from providing reactive power support [3,4]. For example, the German grid code [5] now requires reactive power support from PV farms. In parallel, reactive power markets are emerging [6–9] with the prospect of expanding the portfolio of products offered by PV farm owners. These trends would benefit consumers too because significant savings in grid operation costs are expected with flexible reactive power support from distributed renewable sources [10,11].

One of the key components of the PV farm is the power electronics converter that converts the power generated in direct current (DC) by the PV panels into the alternating current (AC) electric grid. This converter, usually a voltage source converter (VSC), is an expensive asset, but most of the time,

it is used well bellow its rated power: during nighttime, the converter is idle as there is no irradiance and therefore no active power generation; while during daytime, the converter power follows the solar irradiance cycle and reaches the rated power only just a few minutes per day. The remaining converter capacity could then be used to provide reactive power support to the electric grid.

The use of the PV farm converter to provide reactive power support was called "PV-STATCOM" by [12], where the concept was proposed for nighttime operation when the full converter capacity is available. In [13], it was shown that the use of a PV-STATCOM during nighttime can increase the active power transmission limits without the installation of flexible AC transmission system (FACTS) devices or new expensive transmission lines. Following work from the same authors [14,15] extended the PV-STATCOM concept to daytime operation in scenarios where priority was given to active power generation and only the remaining converter capacity could be used for reactive power support: Ref. [14] used the PV system to provide the necessary reactive power for the steady-state and transient operation of a heat pump and Ref. [15] has shown that daytime active power transmission capacity could also be increased by using a PV-STATCOM.

Reactive power support by VSC-based PV farms is possible thanks to the inherent ability of VSCs to control active and reactive power independently. Several works have discussed PV farms' reactive power control schemes with the constraint of keeping the VSC within its capability limits. The direct power control with space vector modulation (DPC-SVM) of single-stage PV farms with three-phase VSC was discussed by [16,17], the control of two-stage single phase PV farms by [18], the voltage-oriented control (VOC) for three phase single-stage PV farms by [17,19] and the control hardware and strategies for two-stage three-phase PV farms by [17,20], and Ref. [17] also presented a model-based predictive controller (MPC). However, none of these works have dealt with the system losses, nor the technical costs of providing reactive power support. Note that distribution network losses due to reactive power support of PV systems were discussed by [21], where global system losses were evaluated through an active-reactive optimal power flow (A-R-OPF).

In the context of wind energy, a technical-economic discussion of wind farms (WF) providing reactive power support to the grid and a modeling of WF capability based on wind variations were presented by [22].

The work in Ref. [23] presented a method to maximize the reactive power reserves while minimizing system losses, and Ref. [24] presented a method to evaluate the losses focusing on the WF and also an operation strategy to minimize power losses when there is a reactive power dispatch. From an overall grid point of view [11,25–27] presented a reactive power dispatch based on A-R-OPF showing that combined reactive support from WF and energy storage systems could significantly reduce the grid losses. Therefore, as previous works did not deal with the losses from the point of view of the PV farm providing reactive power support, the authors proposed earlier a methodology to evaluate the technical cost of operating a PV farm as a STATCOM for nighttime operation [28,29]. A sequel to the work extended the analysis for daytime operation [30], but focused exclusively on single-stage PV farms and lacked a clear step-by-step methodology.

The objective of this paper is to establish a step-by-step methodology to obtain the reactive power support capability map and the associated technical costs of single- and two-stage PV farms for daytime operation. The proposed method relies exclusively on simulations and manufacturer data instead of experimental data. It is assumed throughout this study that priority is given to active power generation, and therefore, only the remaining converter capacity can be used for reactive power support. This work should benefit PV farm owners to plan their bids in future reactive power markets accordingly and to system operators to evaluate if the price paid for this ancillary service is adequate.

This work is structured as follows: Section 2 presents the single- and two-stage PV farm systems used in this work; Section 3 presents the proposed methodology; Section 4 presents the system losses without reactive power support; Section 5 presents the reactive power support capability and the system losses with reactive power support and derives the technical cost of providing the reactive power support.

2. PV Farm Models

This section presents the single- and two-stage PV farms models used throughout this work.

2.1. Single-Stage PV Farm Model

A single-stage PV farm is a topology where only one DC/AC converter is used to interface the PV panel array to the electric grid [31–33]. The DC/AC converter is typically a VSC. Single-stage PV farms are usually more efficient than two-stage ones, but the PV panels' output voltage is not fully decoupled from the grid voltage.

In this work, we adopt the single-stage PV farm shown in Figure 1, which is based on [33]. The DC/AC converter is a two-level, three-phase VSC. The DC/AC converter is connected to the grid through an RL reactor, an RLC series filter to smooth current harmonics and a step-up Δ-Y_g transformer to insulate the PV farm from zero sequence current faults that might occur on the grid side. The system dimensioning and DC/AC controller tuning were presented in [28]. The AC/DC converter controls the PV voltage v_{pv} via a perturb and observe MPPT algorithm [34], as well as the reactive power injected to the grid. The single-stage PV farm parameters are summarized in Table 1. The power-voltage characteristics of the PV panel are shown in Figure 2.

In Figure 1, v_{pv} indicates the PV panel voltage whose reference value is generated by the maximum power point tracker (MPPT) algorithm; C is the capacitor of the DC circuit; i_{abc} is the converter AC current; r_r and L_r are the resistance and the inductance of the tie reactor; R_f, L_f and C_f are the resistance, the inductance and the capacitance of the filter. Both active and reactive power are considered positive when flowing from the PV system to the grid.

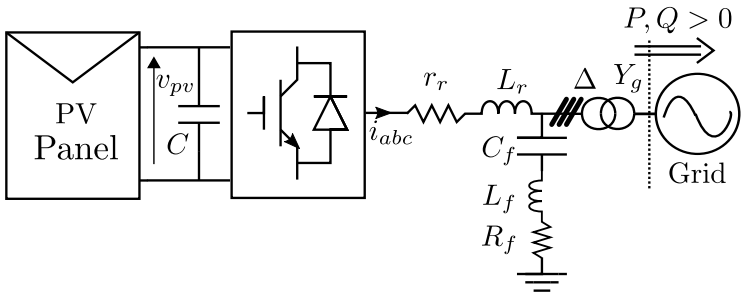

Figure 1. Overview of the single-stage PV system.

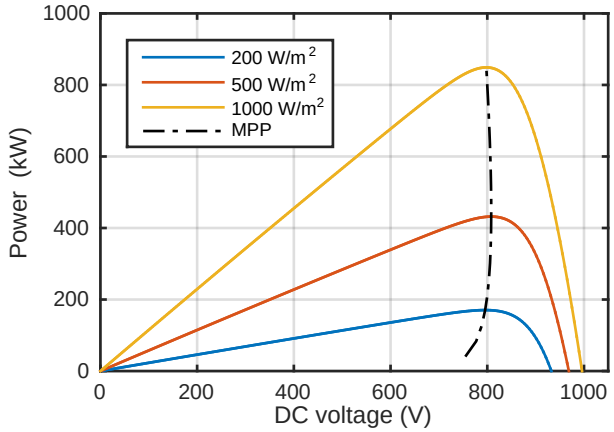

Figure 2. Power-voltage characteristics of the single-stage PV farm PV panel at 25 °C.

Table 1. Single-stage PV farm system parameters.

Parameter	Value	Unit	Parameter	Value	Unit	Parameter	Value	Unit
Rated power	850	kW	v_Δ	380	V	R_f	0.5	Ω
v_{pv} @1000 W/m^2	798	V	f	50	Hz	L_f	397.8	µH
C	87.8	mF	r_r	1	mΩ	C_f	0.64	µF
			L_r	54.1	µH			
Component	**Reference**			**Series modules**		**Parallel modules**		**Total**
PV module	Kyocera Solar KD205GX-LP			30		138		4.140
DC/AC converter	ABB 5SNA1600N170100 IGBT			1		2		12

2.2. Two-Stage PV Farm Model

A two-stage PV farm is a topology where a combination of DC/DC converter(s) and DC/AC converter(s) is used to interface the PV panel to the electric grid [32,35]. Here, again, the DC/AC converter is usually a VSC. The DC/DC converter topology varies depending on the requirements, but its main role is always to decouple the panels' output voltage from the grid voltage, at the cost of higher power losses.

In this work, we adopt the two-stage PV farm shown in Figure 3, which is based on [31,32]. The DC/AC converter is a two-level three-phase VSC, and the DC/DC converter is a boost converter. Again, the DC/AC converter is connected to the grid through an RL reactor, an RLC series filter and a step-up Δ-Y_g transformer. The system dimensioning and the DC/AC converter controller tunings were presented in [28]. The AC/DC converter controls the DC voltage v_{dc} and the reactive power injected to the grid. The DC/DC converter controls the PV voltage v_{pv} via a perturb and observe MPPT algorithm [34]. The two-stage PV farm parameters are summarized in Table 2. The power-voltage characteristics of the PV panel are shown in Figure 4.

In Figure 3, v_{pv} is the PV panel voltage whose reference value is generated by the maximum power point tracker (MPPT) algorithm; v_{dc} is the output voltage of the DC/DC; C_{pv} and C are the DC circuit capacitors; L_{DC} is the DC/DC converter inductor and r_{DC} its resistance; i_{abc} is the converter AC current; r_r and L_r are the resistance and the inductance of the tie reactor; R_f, L_f and C_f are the resistance, the inductance and the capacitance of the filter. Both active and reactive power are considered positive when flowing from the PV system to the grid.

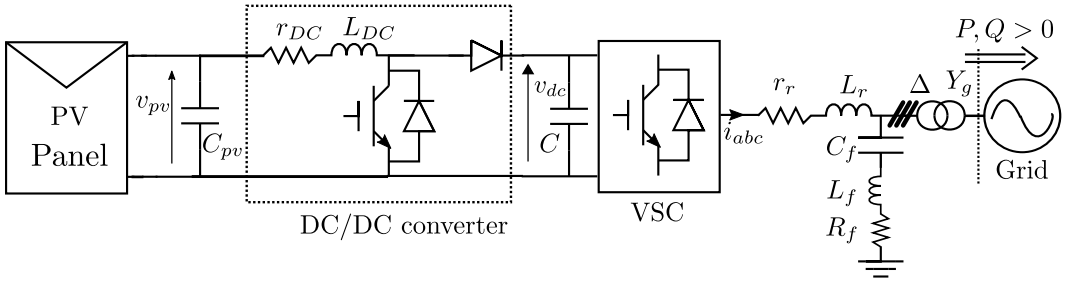

Figure 3. Overview of the two-stage PV system. VSC, voltage source converter.

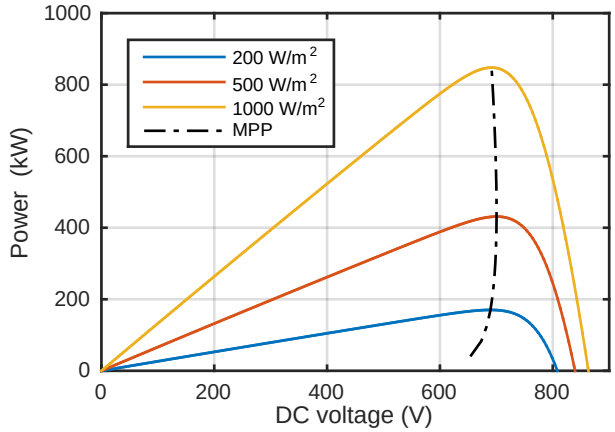

Figure 4. Power-voltage characteristics of the two-stage PV farm PV panel at 25 °C.

Table 2. Two-stage PV farm system parameters.

Parameter	Value	Unit	Parameter	Value	Unit	Parameter	Value	Unit
Rated power	850	kW	v_Δ	380	V	f	50	Hz
v_{pv} @ 1000 W/m^2	691	V	r_{DC}	1	mΩ	R_f	0.5	Ω
C, C_{pv}	87.8	mF	L_{DC}	5.0	mH	L_f	397.8	µH
r_r	1	mΩ	L_r	54.1	µH	C_f	0.64	µF

Component	Reference	Series modules	Parallel modules	Total
PV module	Kyocera Solar KD205GX-LP	26	159	4.134
DC/DC converter	ABB 5SNA1600N170100IGBT	1	1	1
DC/AC converter	ABB 5SNA1600N170100IGBT	1	2	12

3. Methodology

For a given PV farm topology, the goal of this work is to evaluate the reactive power support capability and the associated losses during daytime for a wide range of operating points. Later on, the technical costs can be derived. We assume that priority is given to active power generation; therefore, only the remaining converter capability can be used for reactive power support.

3.1. Flowcharts

The flowcharts presented in Figures 5 and 6 summarize the proposed methodology for evaluating the losses and the reactive power capability for single-stage and two-stage PV farms, respectively. In the following paragraphs, these flowcharts are detailed.

For the single-stage PV farm, the goal is to cover the whole range of operating points (G, Q_{ref}) where G is the solar irradiance and Q_{ref} is the required reactive power support. To initiate the flowchart of Figure 5, the irradiance is set to zero, while Q_{ref} is set to Q_{min}. Then, a simulation for the operating point (G, Q_{ref}) is performed. The next step consists of checking the controls: if the controller references are properly tracked, then the operating point is within the reactive power support capability area, and the power losses are evaluated. Otherwise, if the system controller references are not properly tracked, one of the converter capability limits is violated, and the operating point is outside of the capability area. After the losses evaluation, Q_{ref} is increased by ΔQ until Q_{max} is reached. To restart the evaluation for a new set of operating points, the irradiance G is increased by ΔG, and the procedure is repeated until the maximum local irradiance G_{max} is reached. It is assumed in the simulations that the PV panel temperature is constant at 25 °C.

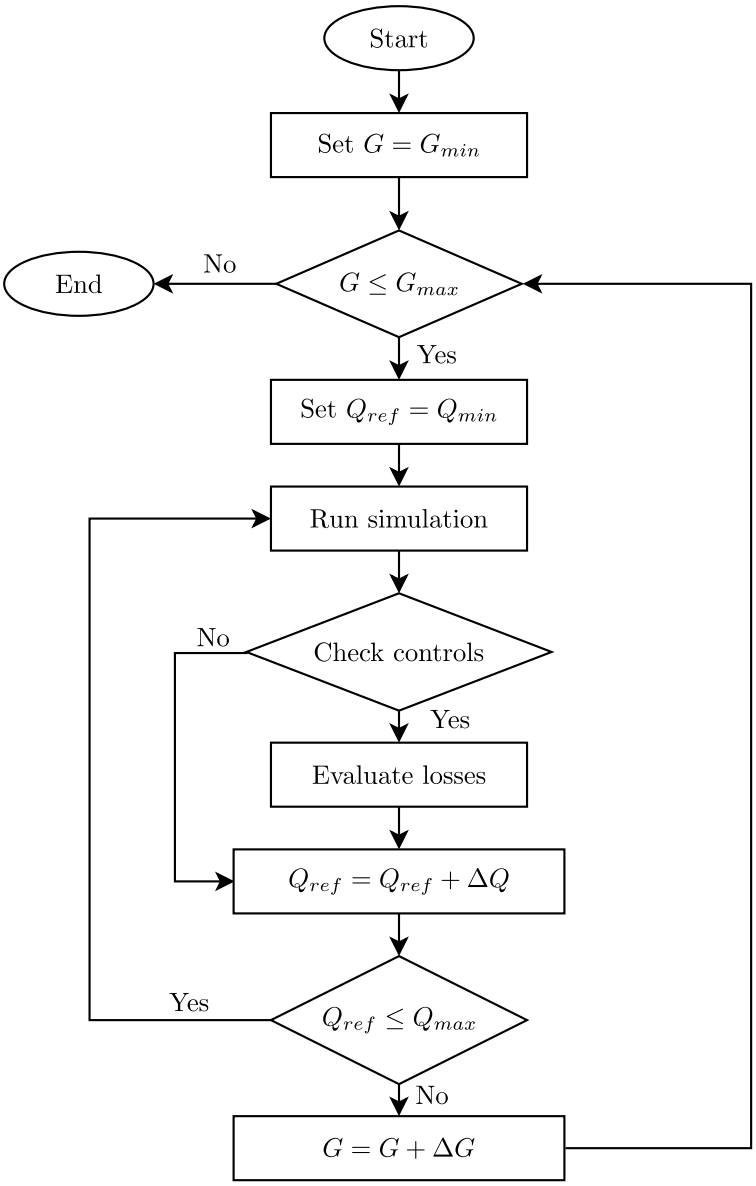

Figure 5. Methodology for the evaluation of daytime losses for single-stage PV farms.

For the two-stage PV farm, the procedure is similar to the previous one, but because of the extra degree of freedom offered by the use of the DC/DC converter, the flowchart presents an extra loop shown in red in Figure 6. Indeed, the DC voltage applied to the DC/AC converter v_{dc} is not tied to the maximum power point (MPP) voltage, meaning that it can be set arbitrarily by the PV farm operator to reduce the DC/AC converter losses [36], for example. Therefore, the goal here is to cover the whole range of operating points (G, v_{dc}, Q_{ref}). Initially, the DC/DC converter output voltage v_{dc} is set to $v_{dc\ min}$, then the procedure is similar to the one of the single-stage PV farm. To move on to the next operating point, v_{dc} is increased by Δv_{dc}, and the procedure is repeated until $v_{dc\ max}$ is reached. The minimum DC circuit voltage is defined as [37]:

$$v_{dc\ min} = x\frac{2\sqrt{2}}{\sqrt{3}}v_{\Delta} \tag{1}$$

where x is taken as 1.15 [38] and v_Δ is the RMS line-to-line voltage at the connection of the VSC output. The maximum DC voltage $v_{dc\ max}$ is taken close to the PV panel open circuit voltage for the maximum local irradiance at −10 °C [39].

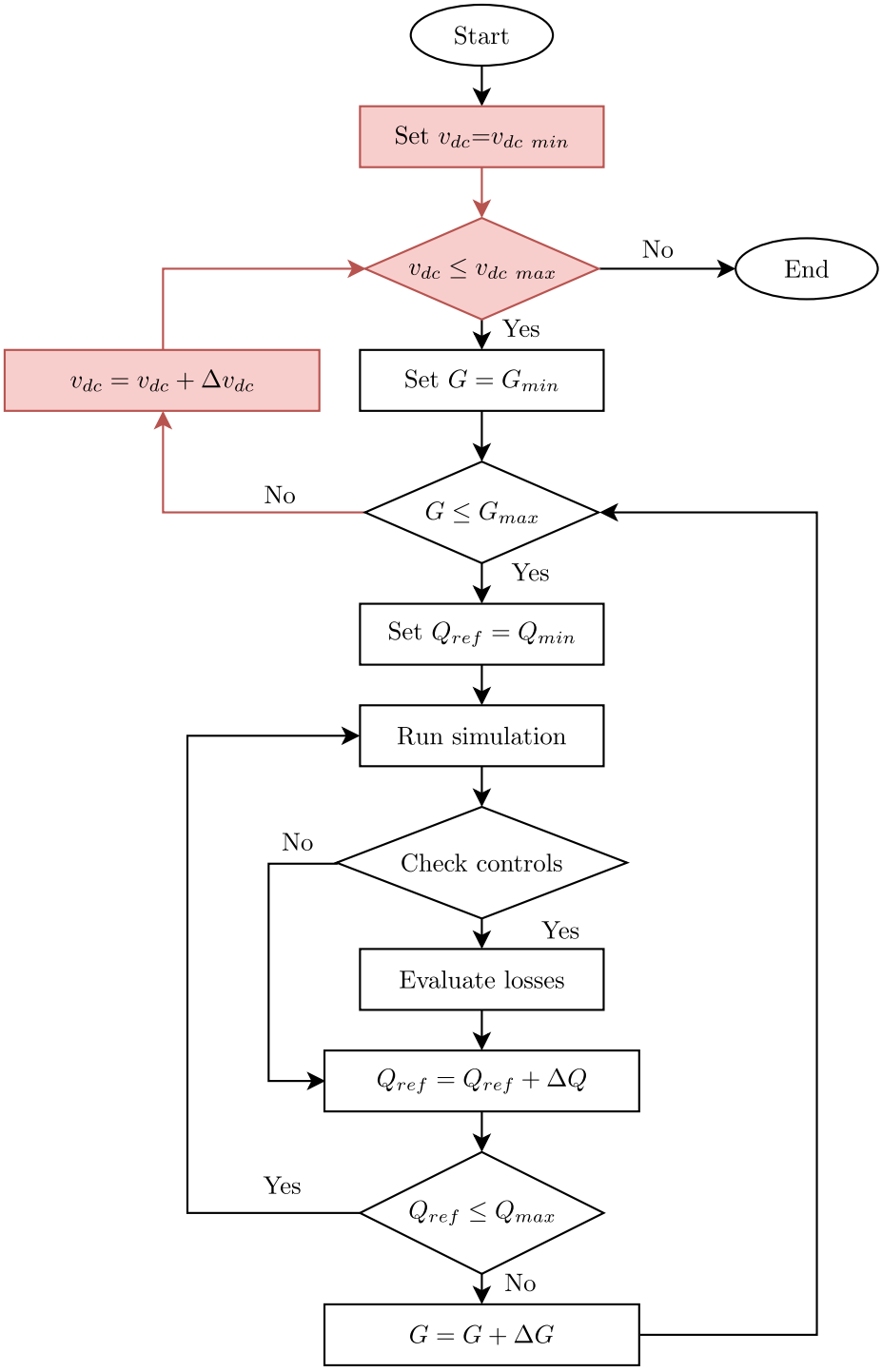

Figure 6. Methodology for the evaluation of daytime losses for two-stage PV farms.

3.2. PV System Losses

For a given operating point, the PV system losses P_{total} are calculated as:

$$P_{total} = (P_{DC/DC}) + P_{DC/AC} + P_{reactor} + P_{filter} + P_{transformer} \quad (2)$$

$P_{reactor}$ and P_{filter} are the Joule losses of the air-cored reactor and of the air-cored filter:

$$P_{reactor} = 3r_r I_r^2 \quad (3)$$

$$P_{filter} = 3R_f I_f^2, \quad (4)$$

where I_r is the reactor current and I_f is the filter current. r_r and R_f are the reactor resistance and filter resistance, respectively.

$P_{transformer}$ is the transformer losses, which can be divided into iron losses P_{iron} and copper losses P_{copper}:

$$P_{transformer} = P_{copper} + P_{iron} \quad (5)$$

with:

$$P_{copper} = 3r_h I_h^2 + 3r_l I_l^2 \quad (6)$$

$$P_{iron} = 3\frac{V_g^2}{R_p} \quad (7)$$

where I_h and I_l are the high and low voltage winding currents and V_g is the line-to-neutral voltage applied to the transformer high voltage windings. r_h, r_l and R_p are the high and low voltage windings' resistances and the iron losses' resistance [40], respectively.

For the DC/DC converter, $P_{DC/DC}$ can be written as:

$$P_{DC/DC} = P_r + P_{IGBT} + P_{diode} \quad (8)$$

where P_r is the DC/DC converter air-cored inductor Joule loss, P_{IGBT} is the IGBT loss and P_{diode} is the diode loss. P_r is calculated as:

$$P_r = r_{DC} I_{DC}^2 \quad (9)$$

where r_{DC} is the air-cored inductor resistance and I_{DC} is the DC bus current.

The losses of the semiconductor devices P_{IGBT}, P_{diode} and the losses of the DC/AC converter $P_{DC/AC}$ do not have a closed formulation. The numerical evaluation of the converter losses for a wide range of operating points using a detailed switch model proved to be unfeasible due to the requirements of simulation steps in the order of nanoseconds. Therefore, alternative models were investigated [36,41–45]. The evaluation of these losses was carried out using the look-up table approach proposed by [45] with the same approximation as [28–30]: the junction temperature was assumed constant at 125 °C, so that only manufacturer data are considered instead of experimental data. The look-up table approach consists of comparing the switch currents' values pre and post the switching transitory. This comparison determines whether the switch was turned on or turned off, and the losses of the respective transitory are obtained through the look-up table. Furthermore, if the switch current is greater than zero, than the respective conduction losses are calculated.

3.3. Technical Costs

According to [30], the technical costs of operating a PV farm as a STATCOM during daytime "are associated with the electric power that must be bought from the grid to supply the difference between the system losses with and without reactive power support". Therefore, for a given irradiance,

by subtracting the PV system losses without reactive power support $P_{total}(Q = 0)$ from the losses with reactive power support $P_{total}(Q \neq 0)$, one can derive the technical costs:

$$Technical\ Costs = P_{total}(Q \neq 0) - P_{total}(Q = 0) \tag{10}$$

By setting $Q_{min} = 0$ p.u. and $Q_{max} = 0$ p.u., one can evaluate $P_{no\ support}$ and by setting $Q_{min} = -1.0$ p.u. and $Q_{max} = +1.0$ p.u., one can obtain the daytime reactive power support capability map and the associated $P_{with\ support}$ of the PV systems.

4. Operation without Reactive Power Support

This section presents the results for losses without reactive power support (needed to derive the technical costs) and shows how the addition of the second stage impacts the losses.

4.1. Single-Stage PV Farm Losses without Reactive Power Support

For the single-stage PV farm, the DC voltage is tied to the irradiance following the MPP as shown in Figures 2 and 7. As a result, the losses are only a function of the solar irradiance. For nighttime operation, when the irradiance is 0 W/m^2, the DC voltage must be set to $v_{dc\ min}$ given by Equation (1). For both test systems, this value is 720 V. Figure 8 details the losses per component, while Figure 10 summarizes the losses as a percentage of the rated power . It can be seen that converter losses are predominant and exhibit an approximately linear behavior with respect to the solar irradiance.

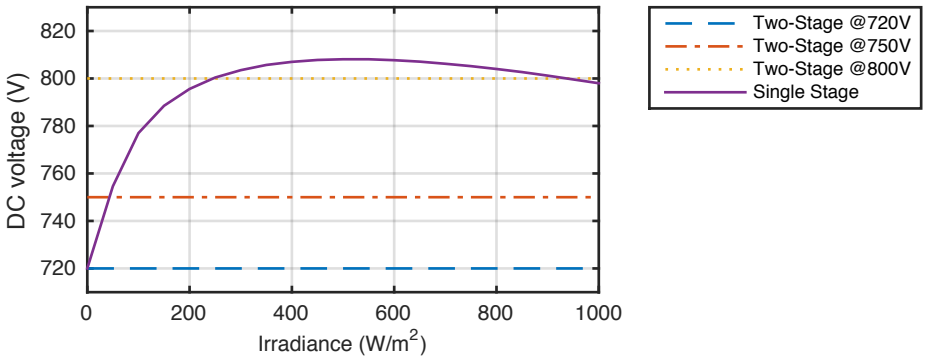

Figure 7. PV farm operating DC voltage v_{dc} as a function of the solar irradiance.

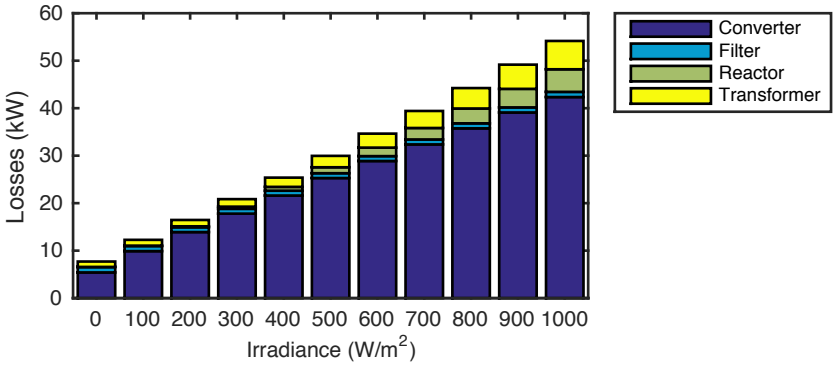

Figure 8. Single-stage PV farm losses per component, without reactive power support. The losses without reactive power support are approximately linear as a function of the irradiance.

4.2. Two-Stage PV Farm Losses without Reactive Power Support

For the two-stage PV farm, the DC voltage can be chosen by the PV farm operator. Three different output DC/DC converter voltages v_{dc} are considered here: 720 V is the minimum voltage for the correct operation of the DC/AC converter; 750 V is the minimum voltage for which the DC/AC converter is able to generate 1.0 p.u. of reactive power support; and 800 V is the voltage at the maximum power point for the standard test conditions (25 °C and 1000 W/m^2) for the single-stage PV farm. Figure 9 details the losses per component.

Figure 10 summarizes the losses as a percentage of the rated power. We observe the same trends as for the single-stage case. The use of the second stage leads to extra losses, but they can be minimized by operating at the lowest DC/DC converter output voltage possible (given by (1)). In the next section, the usefulness of using the second stage will be clarified.

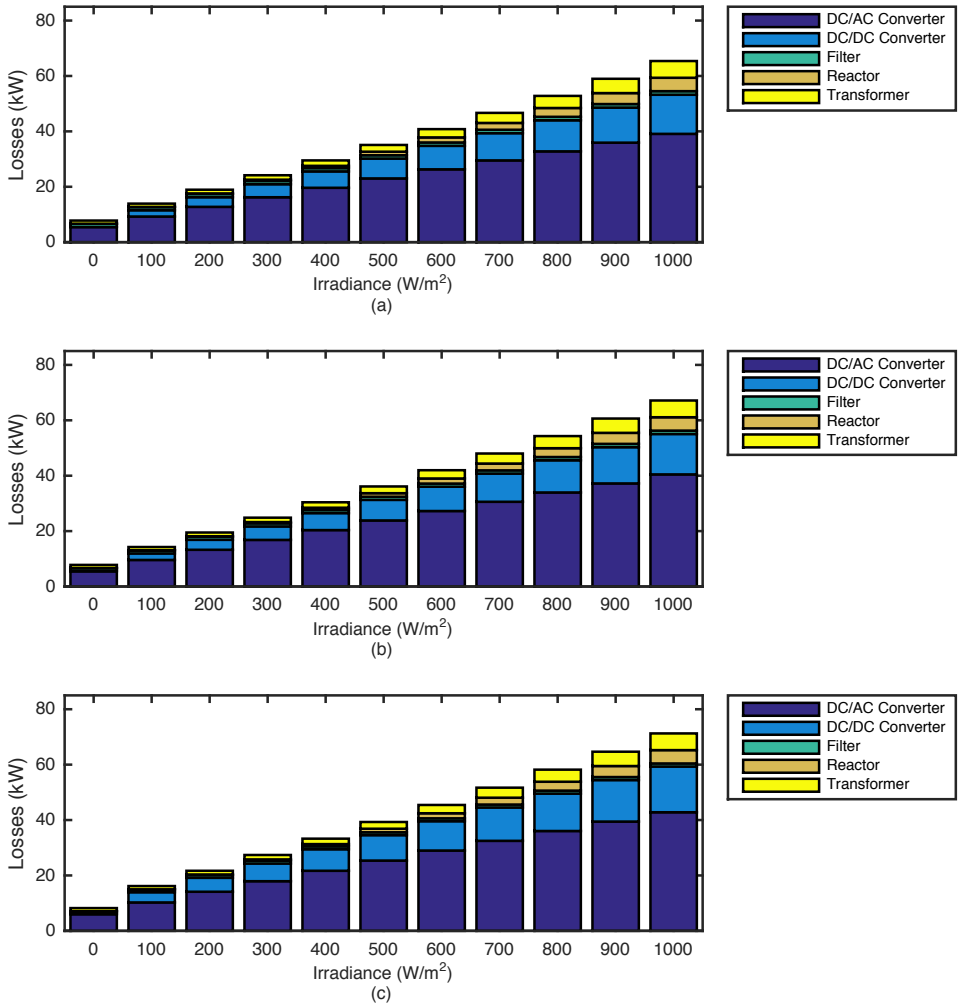

Figure 9. Two-stage PV farm losses per component for various v_{dc}, without reactive power support. (**a**) At 720 V; (**b**) at 750 V; (**c**) at 800 V. The losses without reactive power support are approximately linear as a function of the irradiance.

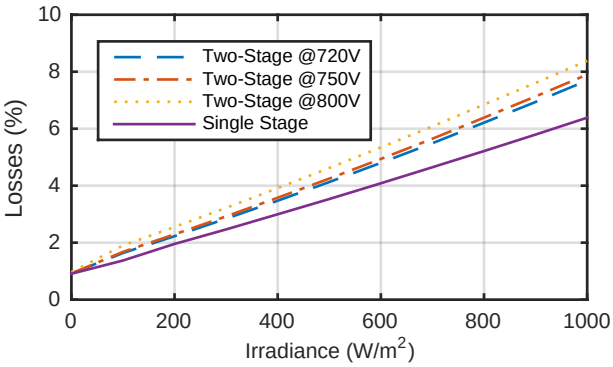

Figure 10. PV farm losses, without reactive power support, as a percentage of the rated power.

5. Operation with Reactive Power Support

This section presents the results regarding reactive power support capability, the evaluated losses for daytime operation with reactive power support and the operation map with the associated technical costs.

5.1. Reactive Power Support Capability Area

We remind that the reactive power support is provided by the DC/AC converter. The PQ-diagram for the 850 kVA DC/AC converter used in both test systems is shown in Figure 11. The circle of radius 1.0 p.u. represents the AC current converter limit, while the arcs represent the AC voltage limit. The AC voltage limit is tied to the DC voltage: a higher DC voltage enables a higher reactive power support capability because the converter is able to synthesize a higher AC voltage [46]. The operating point of the DC/AC converter must be inside those limits.

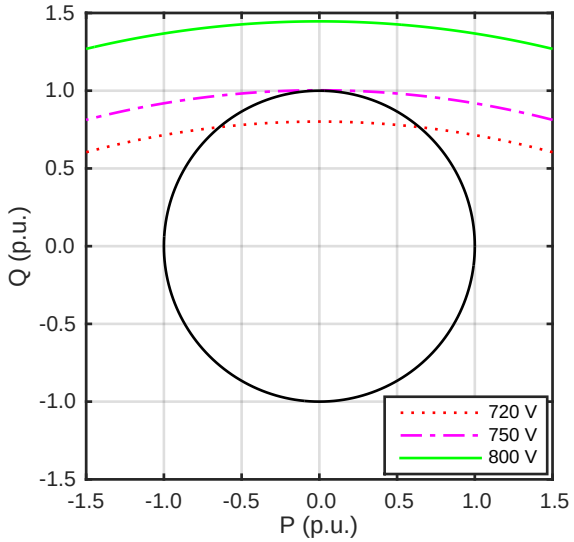

Figure 11. PQ -diagram for the 850 kVA DC/AC converter of both PV farms.

As we focus our analysis on PV farms, in addition to the DC/AC converter limits, one should consider the limits linked to the irradiance. The possible operating points of the DC/AC converter of a PV farm is then better visualized by plotting an GQ-diagram as shown in Figure 12.

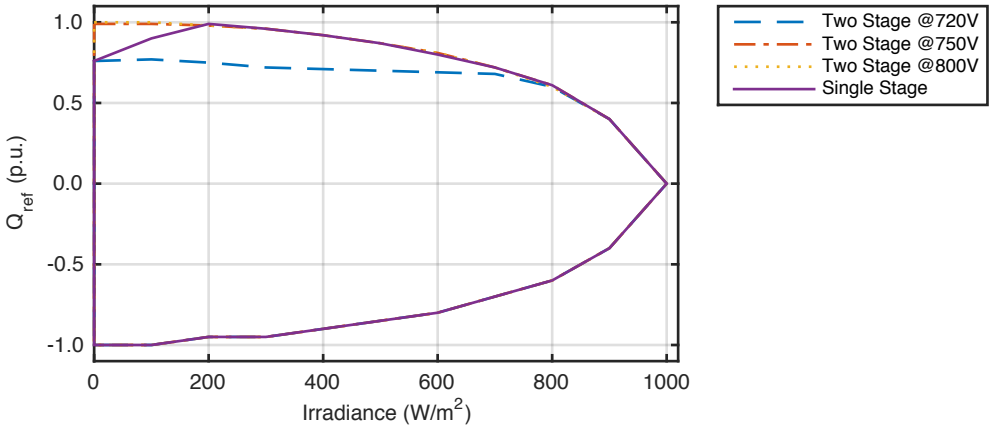

Figure 12. Reactive power support capability area of both PV farms.

For the single-stage PV farm, the reactive power support capability is reduced for irradiance values below 200 W/m^2. This is because the MPPT algorithm generates a low voltage reference $v_{dc\ ref}$ for low irradiance values (according to Figure 7). For irradiance values above 200 W/m^2, the reactive power support is only limited by the AC current converter limit. To extend the reactive power support for low irradiance, one could consider a manual control of the DC voltage, but the system would not operate anymore at the MPP.

For the two-stage PV farm operating at v_{dc} equal to 720 V, the reactive power support is limited compared to the single-stage PV system. However, for v_{dc} equal to 750 V or more, within the converter AC current limit, there is no reactive power support limitation even for low irradiance values. Therefore, the second stage, by decoupling the input DC voltage of the DC/AC converter from the MPP voltage, allows one to extend the reactive power support capability at low irradiance.

5.2. PV Farm Losses with Reactive Power Support

The losses per component can be obtained similarly as before for various reactive power references. At 500 W/m^2, for example, Figures 13 and 14 show the losses for the PV systems as a function of the reactive power references. We observe that the losses increase approximately symmetrically with respect to $|Q_{ref}|$ and that the converter losses are always predominant.

5.3. Technical Cost for Reactive Power Support

Figure 15 shows the technical costs for 500 W/m^2 as an example. Note that because of the AC current limit, one cannot provide 1 p.u. of reactive power at this operating condition. The technical costs of operating the single-stage PV farm and the two-stage PV farm with v_{dc} set to 800 V are approximately equal. Moreover, the cost of operating the two-stage PV farm with v_{dc} set to 720 V or 750 V is slightly higher than the cost of operating it at 800 V. Similar results have been obtained for all irradiance values (not shown here).

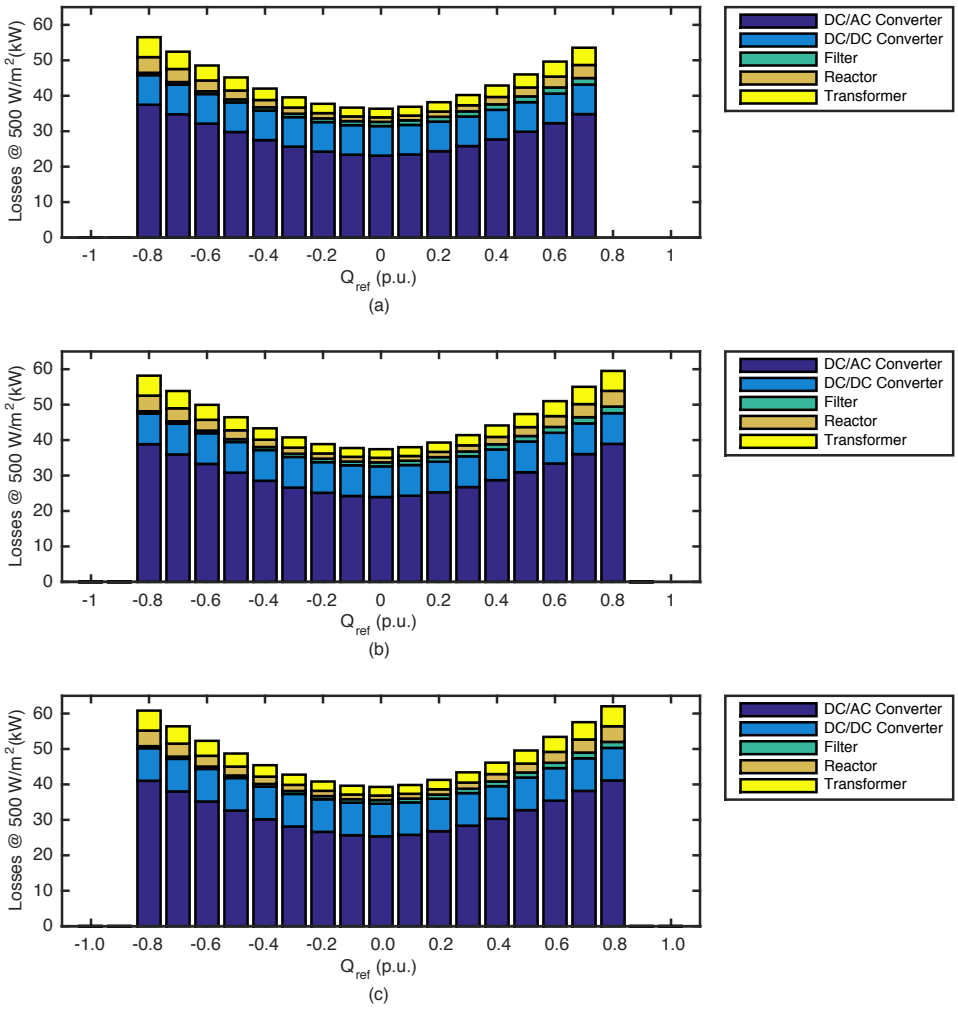

Figure 13. Two-stage PV farm losses per component at 500 W/m^2 for various v_{dc}, with reactive power support. (**a**) At 720 V; (**b**) at 750 V; (**c**) at 800 V. The losses with reactive power support are approximately a quadratic function of the reactive power reference value.

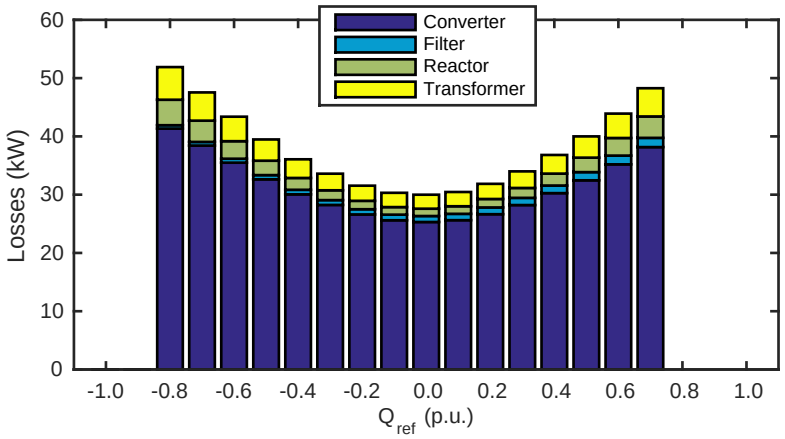

Figure 14. Single-stage PV farm losses per component at 500 W/m^2, with reactive power support. The losses with reactive power support are approximately a quadratic function of the reactive power reference value.

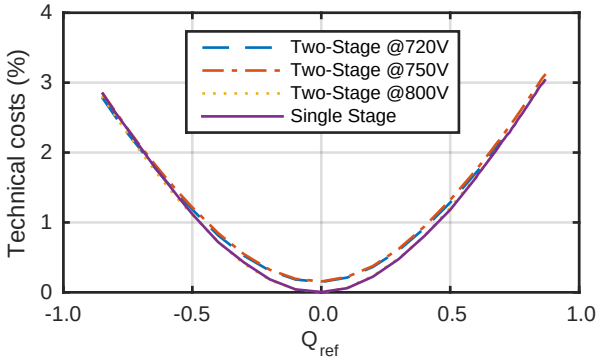

Figure 15. Technical costs of providing reactive power support at 500 W/m^2 for both PV farms, as a percentage of the rated power. Despite losses from two-stage PV farms being higher, the technical costs are similar for both topologies.

By evaluating the technical costs for each point inside the reactive power capability area, one can obtain the maps of Figure 16. One can note that even if the losses of the two-stage PV farm are higher than the ones of the single-stage system, the technical costs of providing reactive power support are similar: they reach 5.1% for the single-stage system and 5.6% for the two-stage system for the worst operating point. These maps underline another point: the cost of providing reactive power is higher at low irradiance than at high irradiance.

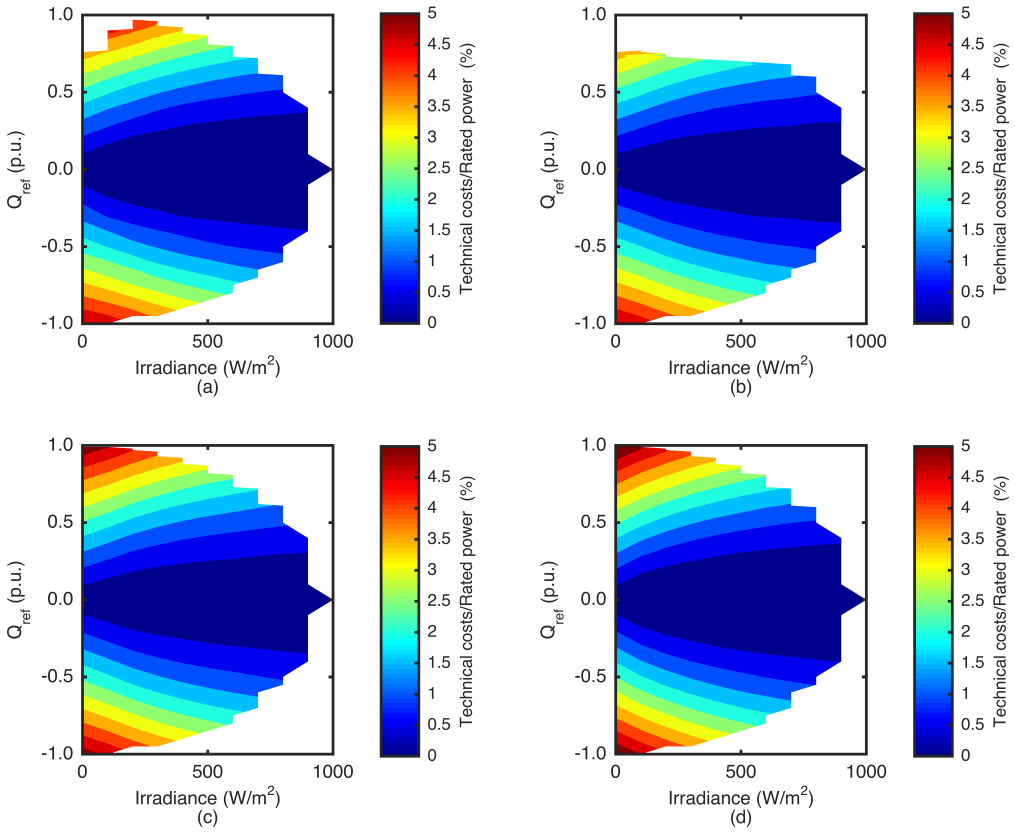

Figure 16. Reactive support capability areas with associated technical costs: (**a**) Single-stage; (**b**) Two-stage at 720 V; (**c**) Two-stage at 750 V; (**d**) Two-stage at 800 V. At 1000 W/m^2, there is no reactive power capability since full converter capacity is being used to inject active power.

5.4. Reactive Power Support Economics

The maps presented in the previous subsection can then be used to estimate the profits of a PV farm providing reactive power support to the grid. To illustrate, we have considered a PV farm located in the Brazilian northeastern region. The hourly average solar irradiance data for a random day was obtained using the Vortex Solar Series satellite data package, and the reactive power dispatch was obtained from [47]. These data are shown in Figure 17. The base value considered for the solar irradiance is 1000 W/m^2 and for reactive power is 850 kVAr.

The Brazilian system operator pays for the reactive power support as an ancillary service. The standard remuneration for this service is 6.88 BRL/MVArh [48] (1 USD = 3.92 BRL). Moreover, at the last energy auction, the average price of the energy sold by PV farms was 145.68 BRL/MWh, which we have considered as the cost for energy losses to estimate the expense generated by the reactive power support. Considering the scenario presented in Figure 17, the evaluation of the reactive power support economic feasibility is presented in Table 3.

The reactive energy demand is obtained by integrating the reactive power dispatch in Figure 17. The technical costs are obtained from the maps in Figure 16 and are shown in Figure 18. By integrating the data in Figure 18, the technical costs can be obtained in MWh. From the results presented exclusively for the reactive power support operation, the two-stage PV farm operating at 720 V is the most profitable for this specific dispatch and daily irradiance cycle.

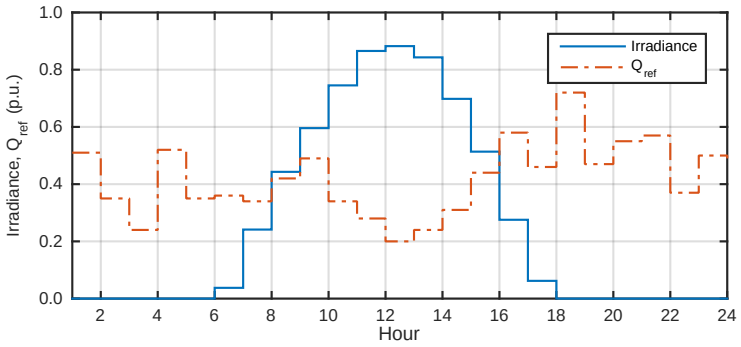

Figure 17. Hourly average solar irradiance data and reactive power dispatch for estimation of the reactive power support revenue. The base value considered for the solar irradiance is 1000 W/m^2 and for reactive power is 850 kVAr.

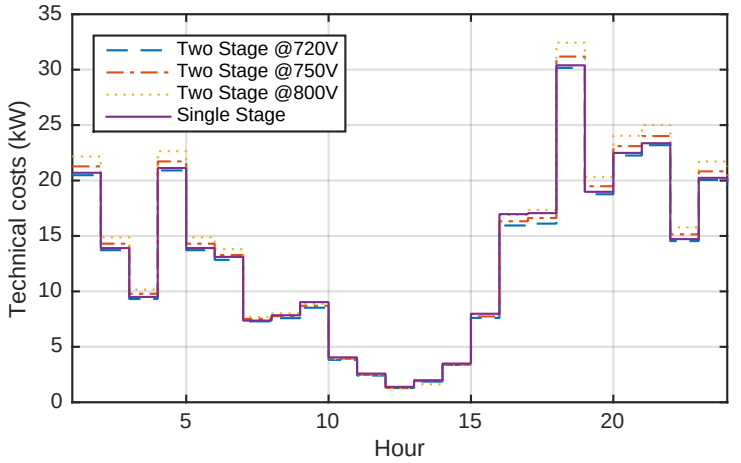

Figure 18. Technical costs for the test systems following the reactive power dispatch and daily irradiation cycle presented in Figure 17.

Table 3. Reactive power support economic feasibility evaluation. Revenue, expenses and profit are expressed in BRL.

Test System	Reactive Power (MVArh)	Technical Costs (MWh)	Revenue	Expenses	Profit
Single-stage	8.59	0.046	59.06	46.53	12.16
Two-stage @720V	8.59	0.045	59.06	45.57	13.12
Two-stage @750V	8.59	0.047	59.06	47.18	11.51
Two-stage @800V	8.59	0.049	59.06	48.93	9.75

As the reactive power markets develop, more complex analysis should be made by the PV farm operators. With dynamic reactive power pricing, more options are available for the PV farm operator to expand the product portfolio. The results presented in this work are the first steps towards analysis that do not feature active power priority, but a compromise between the active and reactive power prices looking to maximize the PV farm profits.

6. Conclusions

As energy mixes worldwide move away from the conventional carbon-emitting sources, PV farms arise as an environmentally-friendly option. In this work, we have presented a step-by-step methodology to evaluate the reactive power support capability and the associated technical costs for single- and two-stage PV farms operating in the daytime. The methodology consists of sweeping a wide range of operating points to help PV farm owners plan their bidding strategies for the reactive power markets that are under discussion. It was shown that the use of the two-stage PV farm allows an improved reactive power support for irradiance values lower than 200 W/m^2. For higher irradiance values, the converter AC current is the limiting factor if the priority is given to active power generation. It was underlined that even if the losses are higher for the two-stage topology in comparison to single-stage PV farms, the technical costs of providing reactive power are quite similar. They reached 5.1% and 5.6% for the single-stage and two-stage PV farms, respectively. Based on the operation maps with reactive power support, it was demonstrated how the profits can be evaluated for a specific dispatch according to the current Brazilian ancillary services policy. These results are interesting to PV farm owners, and during the planning phase, they could be used to determine the best topology: if the revenue provided by reactive power support compensates the technical costs and the extra losses linked to the DC/DC converter, then the two-stage PV farm should be selected.

Author Contributions: Luís F. N. Lourenço proposed the test system, ran the simulations and processed the results; Luís F. N. Lourenço, Renato M. Monaro, Maurício B.C. Salles, José R. Cardoso and Loïc Quéval discussed and validated the methodology; Luís F. N. Lourenço, Renato M. Monaro, Maurício B.C. Salles, José R. Cardoso and Loïc Quéval analyzed and discussed the results; Luís F. N. Lourenço, Renato M. Monaro, Mauricio B. C. Salles and Loïc Quéval wrote the paper.

Funding: This work was supported by São Paulo Research Foundation (FAPESP) grant # 2014/05261-0, by the Brazilian National Research Council (CNPq) grant # 2017-1/06628,and by the Coordination for the Improvement of Higher Education Personnel (CAPES).

Acknowledgments: The authors would like to thank the Brazilian National Research Council (CNPq) and the Coordination for the Improvement of Higher Education Personnel (CAPES) for their financial support.

Conflicts of Interest: The authors declare no conflict of interest.

References

1. SolarPower Europe. *Global Market Outlook for Solar Power 2015–2019*; Technical Report; Euoropean Photovoltaic Industry Association: Bruxelles, Belgium, 2015.
2. Quitmann, E.; Erdmann, E. Power system needs—How grid codes should look ahead. *IET Renew. Power Gener.* **2014**, *9*, 3–9. [CrossRef]

3. Industrial Standards Committee. *IEEE Standard for Interconnecting Distributed Resources with Electric Power Systems*; IEEE Standard 1547; Institute of Electrical and Electronics Engineers: New York, NY, USA, 2003.
4. European Standard. *Voltage Characteristics of Public Distribution Systems*; EN Standard 50160; EN: Bruxelles, Belgium, 2004.
5. Technischen Richtlinie Erzeugungsanlagen am Mittelspannungsnetz. Richtlinie für Anschluss und Parallelbetrieb von Erzeugungsanlagen am Mittelspannungsnetz. Available online: http://www.mega-monheim.de/assets/bdew_rl_ea-am-ms-netz_juni_2008_end.pdf (accessed on 12 June 2018).
6. Gil, J.B.; San Román, T.G.; Rios, J.A.; Martin, P.S. Reactive power pricing: A conceptual framework for remuneration and charging procedures. *IEEE Trans. Power Syst.* **2000**, *15*, 483–489.
7. Thomas, R.J.; Mount, T.D.; Schuler, R.; Schulze, W.; Zimmerman, R.; Alvarado, F.; Lesieutre, B.C.; Overholt, P.N.; Eto, J.H. Efficient and reliable reactive-power supply and consumption: Insights from an integrated program of engineering and economic research. *Electr. J.* **2008**, *21*, 70–81. [CrossRef]
8. Chattopadhyay, D.; Chakrabarti, B.B.; Read, E.G. A spot pricing mechanism for voltage stability. *Int. J. Electr. Power Energy Syst.* **2003**, *25*, 725–734. [CrossRef]
9. Amjady, N.; Rabiee, A.; Shayanfar, H. Pay-as-bid based reactive power market. *Energy Convers. Manag.* **2010**, *51*, 376–381. [CrossRef]
10. Hinz, F.; Moest, D. Techno-economic Evaluation of 110 kV Grid Reactive Power Support for the Transmission Grid. *IEEE Trans. Power Syst.* **2018**. [CrossRef]
11. Gabash, A.; Li, P. Active-reactive optimal power flow in distribution networks with embedded generation and battery storage. *IEEE Trans. Power Syst.* **2012**, *27*, 2026–2035. [CrossRef]
12. Varma, R.K.; Khadkikar, V.; Seethapathy, R. Nighttime application of PV solar farm as STATCOM to regulate grid voltage. *IEEE Trans. Energy Convers.* **2009**, *24*, 983–985. [CrossRef]
13. Varma, R.K.; Rahman, S.A.; Mahendra, A.; Seethapathy, R.; Vanderheide, T. Novel nighttime application of PV solar farms as STATCOM (PV-STATCOM). In Proceedings of the IEEE Power and Energy Society General Meeting, San Diego, CA, USA, 22–26 July 2012; pp. 1–8.
14. Varma, R.K.; Das, B.; Axente, I.; Vanderheide, T. Optimal 24-hr utilization of a PV solar system as STATCOM (PV-STATCOM) in a distribution network. In Proceedings of the IEEE Power and Energy Society General Meeting, San Diego, CA, USA, 24–29 July 2011; pp. 1–8.
15. Varma, R.K.; Rahman, S.A.; Vanderheide, T. New control of PV solar farm as STATCOM (PV-STATCOM) for increasing grid power transmission limits during night and day. *IEEE Trans. Power Deliv.* **2015**, *30*, 755–763. [CrossRef]
16. Mulolani, F.; Armstrong, M.; Zahawi, B. Modeling and simulation of a grid-connected photovoltaic converter with reactive power compensation. In Proceedings of the 9th International Symposium on Communication Systems, Networks & Digital Signal Processing (CSNDSP), Manchester, UK, 23–25 July 2014; pp. 888–893.
17. Romero-Cadaval, E.; Francois, B.; Malinowski, M.; Zhong, Q.C. Grid-connected photovoltaic plants: An alternative energy source, replacing conventional sources. *IEEE Ind. Electron. Mag.* **2015**, *9*, 18–32. [CrossRef]
18. Albuquerque, F.L.; Moraes, A.J.; Guimarães, G.C.; Sanhueza, S.M.; Vaz, A.R. Photovoltaic solar system connected to the electric power grid operating as active power generator and reactive power compensator. *Sol. Energy* **2010**, *84*, 1310–1317. [CrossRef]
19. Samadi, A.; Ghandhari, M.; Söder, L. Reactive power dynamic assessment of a PV system in a distribution grid. *Energy Procedia* **2012**, *20*, 98–107. [CrossRef]
20. Blaabjerg, F.; Teodorescu, R.; Liserre, M.; Timbus, A.V. Overview of control and grid synchronization for distributed power generation systems. *IEEE Trans. Ind. Electron.* **2006**, *53*, 1398–1409. [CrossRef]
21. Gabash, A.; Li, P. Active-reactive optimal power flow for low-voltage networks with photovoltaic distributed generation. In Proceedings of the 2012 IEEE International Energy Conference and Exhibition (ENERGYCON), Florence, Italy, 9–12 September 2012; pp. 381–386.
22. Ullah, N.R.; Bhattacharya, K.; Thiringer, T. Wind farms as reactive power ancillary service providers—Technical and economic issues. *IEEE Trans. Energy Convers.* **2009**, *24*, 661–672. [CrossRef]
23. Jung, S.; Jang, G. A Loss Minimization Method on a reactive power supply process for Wind Farm. *IEEE Trans. Power Syst.* **2017**, *32*, 3060–3068. [CrossRef]
24. Zhang, B.; Hu, W.; Hou, P.; Tan, J.; Soltani, M.; Chen, Z. Review of Reactive Power Dispatch Strategies for Loss Minimization in a DFIG-based Wind Farm. *Energies* **2017**, *10*, 856.

[CrossRef]
25. Gabash, A.; Li, P. Evaluation of reactive power capability by optimal control of wind-vanadium redox battery stations in electricity market. *Renew. Energy Power Qual. J.* **2011**, 1–6. [CrossRef]
26. Gabash, A.; Li, P. On variable reverse power flow—Part I: Active-Reactive optimal power flow with reactive power of wind stations. *Energies* **2016**, *9*, 121. [CrossRef]
27. Gabash, A.; Li, P. On variable reverse power flow—Part II: An electricity market model considering wind station size and location. *Energies* **2016**, *9*, 235. [CrossRef]
28. Lourenço, L.F.N. Technical Cost of Operating a PV Installation as a STATCOM during Nightime. Master's Thesis, Universidade de São Paulo, São Paulo, Brazil, 2017.
29. Lourenço, L.F.N.; Salles, M.B.C.; Monaro, R.M.; Quéval, L. Technical Cost of Operating a Photovoltaic Installation as a STATCOM at Nighttime. *IEEE Trans. Sustain Energy* **2018**. [CrossRef]
30. Lourenço, L.F.N.; Salles, M.B.C.; Monaro, R.M.; Quéval, L. Technical cost of PV-STATCOM applications. In Proceedings of the 2017 IEEE 6th International Conference on Renewable Energy Research and Applications (ICRERA), San Diego, CA, USA, 5–8 November 2017; pp. 534–538.
31. Blaabjerg, F.; Chen, Z.; Kjaer, S.B. Power electronics as efficient interface in dispersed power generation systems. *IEEE Trans. Power Electron.* **2004**, *19*, 1184–1194. [CrossRef]
32. Kouro, S.; Leon, J.I.; Vinnikov, D.; Franquelo, L.G. Grid-connected photovoltaic systems: An overview of recent research and emerging PV converter technology. *IEEE Ind. Electron. Mag.* **2015**, *9*, 47–61. [CrossRef]
33. Yazdani, A.; Di Fazio, A.R.; Ghoddami, H.; Russo, M.; Kazerani, M.; Jatskevich, J.; Strunz, K.; Leva, S.; Martinez, J.A. Modeling guidelines and a benchmark for power system simulation studies of three-phase single-stage photovoltaic systems. *IEEE Trans. Power Deliv.* **2011**, *26*, 1247–1264. [CrossRef]
34. De Brito, M.A.; Sampaio, L.P.; Luigi, G.; e Melo, G.A.; Canesin, C.A. Comparative analysis of MPPT techniques for PV applications. In Proceedings of the 2011 International Conference on Clean Electrical Power (ICCEP), Ischia, Italy, 14–16 June 2011; pp. 99–104.
35. Huang, L.; Qiu, D.; Xie, F.; Chen, Y.; Zhang, B. Modeling and Stability Analysis of a Single-Phase Two-Stage Grid-Connected Photovoltaic System. *Energies* **2017**, *10*, 2176. [CrossRef]
36. Blaabjerg, F.; Jaeger, U.; Munk-Nielsen, S. Power losses in PWM-VSI inverter using NPT or PT IGBT devices. *IEEE Trans. Power Electron.* **1995**, *10*, 358–367. [CrossRef]
37. Hansen, A.D.; Michalke, G. Modelling and control of variable-speed multi-pole permanent magnet synchronous generator wind turbine. *Wind Energy* **2008**, *11*, 537–554. [CrossRef]
38. Liserre, M.; Blaabjerg, F.; Dell'Aquila, A. Step-by-step design procedure for a grid-connected three-phase PWM voltage source converter. *Int. J. Electron.* **2004**, *91*, 445–460. [CrossRef]
39. Fronius International GmbH Solar Energy Division. *Sizing the Maximum DC Voltage of PV Systems*; Fronius International GmbH Solar Energy Division: Wels, Austria, 2015.
40. Martinez, J.A.; Mork, B.A. Transformer modeling for low-and mid-frequency transients—A review. *IEEE Trans. Power Deliv.* **2005**, *20*, 1625–1632. [CrossRef]
41. Blaabjerg, F.; Pedersen, J.K.; Sigurjonsson, S.; Elkjaer, A. An extended model of power losses in hard-switched IGBT-inverters. In Proceedings of the Conference Record of the 1996 IEEE Industry Applications Conference Thirty-First IAS Annual Meeting (IAS'96), San Diego, CA, USA, 6–10 October 1996; Volume 3, pp. 1454–1463.
42. Rajapakse, A.; Gole, A.; Wilson, P. Electromagnetic transients simulation models for accurate representation of switching losses and thermal performance in power electronic systems. *IEEE Trans. Power Deliv.* **2005**, *20*, 319–327.
43. Wong, C. EMTP modeling of IGBT dynamic performance for power dissipation estimation. *IEEE Trans. Ind. Appl.* **1997**, *33*, 64–71. [CrossRef]
44. Drofenik, U.; Kolar, J.W. A general scheme for calculating switching-and conduction-losses of power semiconductors in numerical circuit simulations of power electronic systems. In Proceedings of the 2005 International Power Electronics Conference (IPEC 9205), Niigata, Japan, 4–8 April 2005; pp. 4–8.
45. Munk-Nielsen, S.; Tutelea, L.N.; Jaeger, U. Simulation with ideal switch models combined with measured loss data provides a good estimate of power loss. In Proceedings of the Conference Record of the IEEE Industry Applications Conference, Rome, Italy, 8–12 October 2000; Volume 5, pp. 2915–2922.
46. Cole, S. Steady-State and Dynamic Modelling of VSC HVDC Systems for Power System Simulation. Ph.D. Thesis, Katholieke Universiteit Leuven, Leuven, Belgium, 2010.

47. Haghighat, H.; Kennedy, S. A model for reactive power pricing and dispatch of distributed generation. In Proceedings of the IEEE Power and Energy Society General Meeting, Providence, RI, USA, 25–29 July 2010; pp. 1–10.
48. Tarifas de Energia de Otimização e de Serviços Ancilares para 2018 (Optimization and Ancillary Services Tariffs for 2018). Available online: http://www.aneel.gov.br/sala-de-imprensa-exibicao-2/-/asset_publisher/zXQREz8EVlZ6/content/fixadas-as-tarifas-de-energia-de-otimizacao-e-de-servicos-ancilares-para-2018/656877?inheritRedirect=false (accessed on 7 June 2018).